Available online at www.sciencedirect.com

ScienceDirect

Proceedings of the Combustion Institute 38 (2021) 3651–3659

Proceedings of the Combustion Institute

www.elsevier.com/locate/proci

Numerical study of self-sustained oblique detonation in a non-uniform mixture

Kazuya Iwata [a,*], Osamu Imamura [b], Kazuhiro Akihama [b], Hiroshi Yamasaki [b], Shinji Nakaya [b], Mitsuhiro Tsue [c]

[a] *Japan Aerospace Exploration Agency, Kakuda 981-1525, Japan*
[b] *Nihon University, Narashino 275-8575, Japan*
[c] *University of Tokyo, Bunkyo-ku, 113-8656, Japan*

Received 8 November 2019; accepted 20 July 2020
Available online 29 September 2020

Abstract

Self-sustained oblique detonation behind a spherical projectile formed in a non-uniform $H_2/O_2/Ar$ mixture was numerically investigated. A hypersonic combustible mixture flow around a 4.76 mm diameter body was modeled to be flowing at 2500 m/s and 100 kPa. The concentration gradient was prescribed applying the Gaussian distribution to hydrogen concentration. Axisymmetric Euler equations including a detailed kinetics of 9 species and 27 elementary reactions were solved with an explicit 2nd-order time integration scheme combined with point implicit method for chemical reaction. Oblique detonation was always obtained when the mixture on the centerline was stoichiometric, as it is for a uniform mixture, and a broader range of equivalence ratio could sustain oblique detonation far from the sphere. Local detonation angle was revealed to reasonably match Chapman-Jouguet analytical solutions with a minor difference attributed to curvature, less reactive composition, and the concentration gradient. Also, a strongly fuel-rich region encountered decoupling of the shock-flame, in which an abrupt deflection of the shock front appeared. These decoupling phenomena can be attributed to a slower kinetics of a less reactive mixture. All of interesting findings in this study will also benefit understanding of various form of detonation in non-uniform mixture taking advantage of the analogy between them.

Keywords: Oblique detonation; Numerical simulation; Hydrogen; Inhomogeneous; Non-uniform

1. Introduction

Oblique detonation wave (ODW) [1] is attracting an increasing attention for its potentiality to a new conceptual high-speed airbreathing vehicle as Oblique Detonation Wave Engine (ODWE) [2–4], in which continuous and steady formation of detonative combustion contributes to improved specific impulse relative to that of scramjet engine especially at higher flight Mach number exceeding M∼15 [2]. Simplified schematic of ODW is illustrated in Fig. 1 for a sphere-induced form [5–8].

* Corresponding author.
E-mail address: iwata.kazuya@jaxa.jp (K. Iwata).

https://doi.org/10.1016/j.proci.2020.07.070

Nomenclature

a	= steepness of the gradients
d	= sphere diameter
D	= detonation velocity
V	= velocity
x	= horizontal position
y	= vertical position
X	= mole fraction
β	= angle of oblique detonation/shock wave [°]
Φ	= equivalence ratio
λ	= cell width
Subscript	
$\mathbb{C}$	= centerline

ODW is steadily stabilized on a body-fixed coordinate, differently from conventionally studied normal detonation. Behind the supporting body, the wave front converges into a planar front which maintains itself as dictated by Chapman–Jouguet (C–J) theory. Therefore, its wave angle β_{CJ} is described through the balance between C–J velocity D_{CJ} and the speed of the flow relative to the body V_p like Eq. (1) below:

$$\beta_{CJ} = \arcsin\left(D_{CJ}/V_p\right) \tag{1}$$

Several characteristic features of ODW including induction region upstream of the transition point to detonation [9–12], several different manners in the transition [9–12], and formation of one-sided transverse wave [13,14] have been motivating researchers to conduct fundamental researches including both experimental [6–8] and numerical [5,9–12] approaches. On the other hand, a recent interest associated with the problem occurring in various forms of detonation engines is about how non-ideal mixing influence the physics of detonation, since a high-frequency operation reaching the order of kHz makes fuel-oxidizer mixing difficult to be completed. It is similarly of a major concern in ODWE where mixing is achieved in hypersonic air flow [15–18], but only a limited number of previous researches have worked on that effect on ODW [18–20]. Interesting morphologies of detonation have been being uncovered including parallelogram-like deformed cell pattern observed by Ishii and Kojima [21], an increased chance for deflagration-to-detonation (DDT) to occur in certain conditions [22], an unexpected increase of propagation velocity due to hot product gas [23], and many other phenomena in the literature [21-24]. On the other hand, only a few qualitative discussions are found on ODW formation [18–20], and recent works by Iwata et al. [25–28] and Fang et al. [29] addressed non-uniformly premixed ODW on a wedge/sphere in a parametric way, but only a few aspects has just started to be understood. Therefore, much more progress is needed to reach comprehensive understanding.

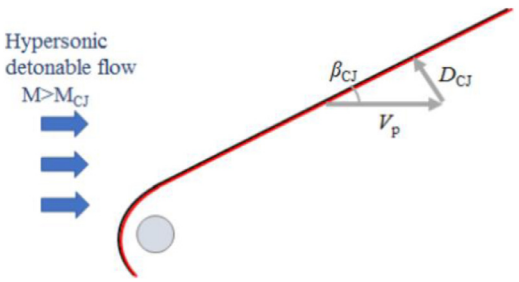

Fig. 1. Schematic image of oblique detonation wave (ODW).

In our previous researches, sphere-/wedge- induced ODW in a non-uniform hydrogen-air mixture was studied, revealing the decoupling of the shock-flame induced by the non-uniformity initiates a locally confined oscillation on a sphere body [25], and V-shaped initiating flame front is formed upstream of wedge-induced ODW in a strong gradient [26,27], which is supported by a subsequent work by Fang et al. [29]. Thus, we have so far addressed mainly body-supported overdriven ODW, whereas C–J self-sustained one has never been addressed. The present study then focuses on self-sustained C-J ODW in a non-uniform mixture, comparing it to that in a uniform mixture and investigating the correspondence of the local wave structure to C–J theoretical properties. Hydrogen/oxygen/argon mixture flow around a spherical body was simulated according to the experimental configurations by Maeda et al. [8] and our ongoing experiments [28].

2. Numerical simulation

As mentioned in the previous section, self-sustained ODW in a non-uniform mixture was presently studied with a numerical approach. A hypersonic combustible flow around a 4.76 mm diameter sphere body [28] was modeled in an axisymmetric fashion as shown in Fig. 2, where 3000×3999 grid distribution is illustrated extending from the front side of the body to the far field in the rear side. Grid size is thus variable depending on the location, with the smallest size 2.54 μm on the centerline, and the largest grid 9.75 μm on the frank of the projectile. By this distribution, 13 grids on the centerline and 5 grids on the frank are placed within half reaction length of stoichiometric detonation. This is relatively coarser than the resolutions in recent numerical works on detonation reaching several tens of grids per induction length, but oblique path in initiation process is considered to rationalize the coarser resolution for ODW simulation [11]; 18 grids are presently contained in

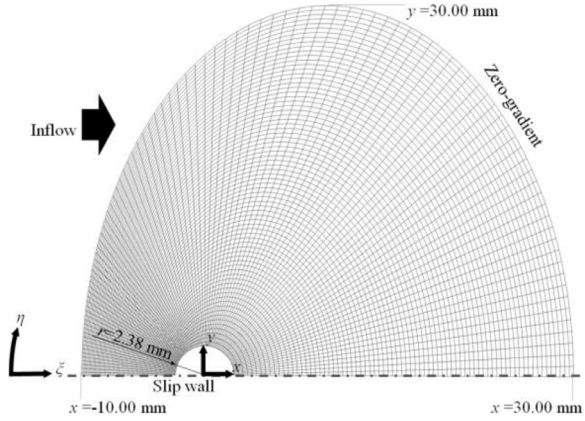

Fig. 2. Computational domain.

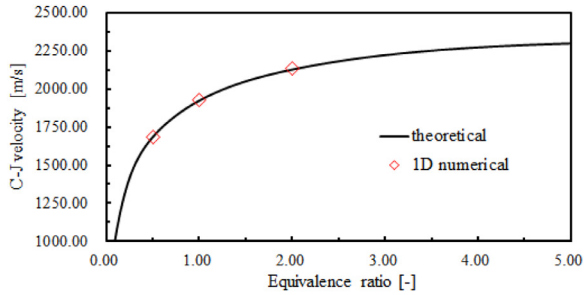

Fig. 3. Variation of C–J velocity of 2Φ H_2+O_2+3Ar mixture.

C–J detonation path before ignition. And since the present focus is on static feature, rather than dynamic cellular structure, higher resolution in the half reaction length is not necessarily important, and the present resolution is justified for discussion on static features including detonation angle/velocity, as shown by grid dependence study. Hydrogen/oxygen/argon mixture flows from the left-hand boundary at V_p=2500 m/s (Mach number $M = 6.62$ for stoichiometric mixture). V_p is set higher than those in the experiments [8,28] to accommodate a wider range of equivalence ratio within the limitation $V_p > D_{CJ}$, as confirmed from Fig. 3 showing theoretical C–J velocity. Since the wave fronts distant from the body is of the main concern in this study, Boundary layer was neglected by using a slip-wall condition on the surface of the body which is not likely to have a major effect on the wave structures. Outflow towards the right-hand boundary can be subsonic perpendicular to it, for which a method of non-reflecting boundary [30] was applied to avoid unphysical disturbance from returning upstream. In the following non-uniform flow simulations, however, subsonic outflow was never experienced including the wake flow behind the sphere, which substantiates that the outlet boundary does not collapse the physical reality of the flow in the entire region.

The concentration gradient was created artificially, by applying the Gaussian function to describe mole fraction of hydrogen:

$$X_{H2} = \begin{cases} X_0 \exp(-ay^2) \\ 1 - X_0 \exp(-ay^2) \end{cases} \quad (2)$$

where the maximum concentration occurs on the centerline in the upper branch formulation, while the minimum on the centerline in the lower. Oxidizer composition was always O_2+3Ar so that the local composition with local equivalence ratio Φ_{local} becomes $2\Phi_{local}$ H_2+O_2+3Ar. Static pressure and static temperature were all matched to the constant values 100 kPa and 300 K, respectively. Centerline local equivalence ratio $\Phi_{\mathfrak{C}}$ was always taken to be unity in all the simulations, and outermost local equivalence ratio Φ_{out} was varied to define X_o and a in Eq. (2) for each non-uniform condition.

Axisymmetric two-dimensional Euler equations were solved as the governing equations, involving 9 species conservation equations. A detailed chemical kinetics proposed by Konnov [31] including 27 elementary reactions was employed to calculate chemical source terms. AUSM+up scheme [32] was used to discretize convection terms, with the use of minmod limiter to realize second-order in space. As will be mentioned, second-order accuracy does not deteriorate the quality of our

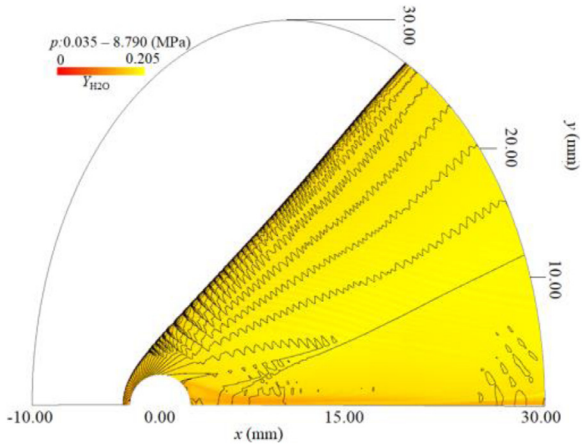

Fig. 4. Overlaid contours of pressure (black lines) and water mass fraction (yellow-red color map) for the uniform case with Φ=1.00, V_p=2500 m/s.

discussion since the cellular structure is presently out of main scope. Temporal integration was implemented in an explicit way with the second-order TVD Runge–Kutta scheme [33], but Point Implicit Method was applied for chemical source term with a full inversion of Jacobian matrix.

3. Results and discussion

3.1. Uniform composition

Uniformly stoichiometric flows with the composition $2H_2+O_2+3Ar$ was in the first place simulated to validate employed numerical methods against well-established experimental observation including scaling law [8,28], and theoretical analysis. The obtained result is illustrated in Fig. 4 as overlaid contours of pressure (black lines) and water mass fraction (color maps) indicating the shock wave and the flame front structures, respectively. A strongly coupled shock-flame is formed in front of a sphere body as an overdriven detonation, then being attenuated into a planar wave front behind it. This success in stabilized ODW agrees with corresponding experimental observations by Iwata et al. [28] and Maeda et al. [8] where self-sustained ODW in $2H_2+O_2+3Ar$ mixture was achieved with a non-dimensional diameter d/λ more than 3.5 (d/λ of the present mixture is 3.7). Unsteady transversal waves appeared around $y\sim5$ mm facing downstream as was observed numerically on a wedge-induced one [13,14], although it apparently varies in the interval along the wave front partly owing to radially variable grid resolution which is known to strongly influence the scale of cellular structure [34], including that of ODW [13,14]. However, as will be proved later, temporally averaged wave front is less grid-dependent, for which static properties of ODW front look to be well captured. Since behavior of detonation cellular structure in numerical study has much remaining to be revealed including its extreme grid dependence, the scope of the present study will be focused on the static behavior of ODW front omitting discussion on cellular dynamics.

In order to compare the wave structures observed here to the theoretical analysis, one-dimensional calculation algorithm equipped as DETON subroutine in CEA program [35] was applied to derive C-J velocity, which in turn was used to calculate theoretical ODW angle β_{CJ} by the use of Eq. (1). β_{CJ} calculated in this way for $2H_2$–O_2–3Ar mixture at V_p=2500 m/s was 50.28°. Actually obtained wave angle in Fig. 4 on the planar part 49.6°, being a good agreement. Therefore, the present simulation well captures static physics of ODW. The little lower angle than CEA analysis is contrary to those in our complementary 1D simulation shown in Fig. 3 using the same discretization schemes for three different equivalence ratios Φ=0.50, 1.00, 2.00, which predicted a little overdriven velocity exceeding C-J value by 5-10 m/s. Therefore, this opposite tendency seems to come from wave attenuation by multi-dimensional curvature.

Another uniformly premixed condition was also simulated with different equivalence ratio Φ=2.00 mixture. It failed in stabilization of ODW, resulting into shock-induced combustion (SIC, not shown here). This result also agrees with our experimental observation [28], and d/λ=1.9 for Φ=2.00 is consistently below the threshold d/λ =3.5. Although other uniform conditions have not been explored, it indicates at least that $\Phi\geq$2.00 cannot form ODW in uniform mixture. This different result will render an important perspective on the threshold for the occurrence of ODW.

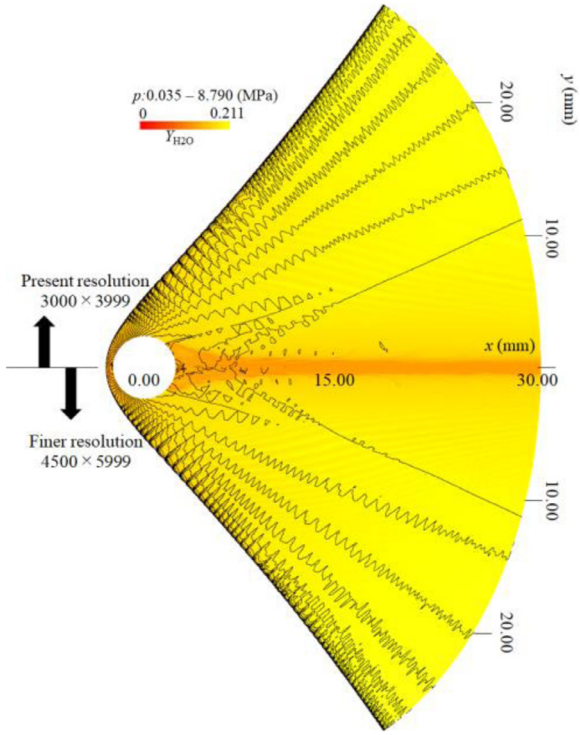

Fig. 5. Grid dependence of ODW structure for Φ_{out}=2.00 case with the basic resolution (upper) and the finer resolution (lower).

3.2. Grid dependence of solution

Another simulation was conducted using one different resolution with the number of grids taken to be one and a half time better in each direction 4500×5999. The simulation results for the case Φ_{out}=2.00 with the basic resolution 3000×3999 and the finer resolution 4500×5999 are illustrated in one picture Fig. 5. Upper half of the contour is from the result by the present grid, and the lower half by the finer one. It is clear that both wave structures predicted excellently match each other. Quantitative pressure distribution is almost coincident, and only minor difference in behavior of transverse wave is found, for example on the location for its initiation, which is closer to the sphere with the finer grid. The interval of transverse wave is smaller for the finer grid, and also dynamic motion of the incident front is better captured.

To study the effect of resolution on static features including local wave angle, which is crucial for subsequent discussion, the location of ODW front and its wave angle distribution were compared in Fig. 6. From Fig. 6(a), the wave structure in an overall perspective is clearly almost identical. A detailed view of local wave angle in Fig. 6(b) versus y-position exhibits a relatively detectible difference, especially close to the initiation of transverse wave resulting in an oscillating behavior partly due to the method for evaluation of the wave angle here: evaluated with local averaging of 5 points on each of which central difference was calculated by $\pm$10 distant points on ODW front. However, averaged behavior of the variation is close to each other, and converged planar region in y>15 mm is identical in the angle distribution, which supports the validity of using the basic resolution for theoretical discussion of ODW using wave angle through Eq. (1). Regardless of minor difference of the wave angle and cell-like pattern observed, one can expect that the basic grid resolution is sufficient to study the static wave structure of ODW and its features in the case of mixtures with concentration gradients. To quantitatively capture cellular dynamics in the future, uniformly aligned grid and higher-order discretization scheme will be needed.

3.3. Non-uniform conditions

Non-uniform distribution of hydrogen (Eq. (2)) was prescribed to the inflow mixture, under the limitation of centerline local equivalence ratio $\Phi_{\mathbb{C}}$ being unity $\Phi_{\mathbb{C}}$=1.00. Outermost local equivalence ratio Φ_{out} at $y = 30.00$ mm was varied in the range 0.25–4.00. The obtained wave structures in five cases of them are illustrated in Fig. 7 in the

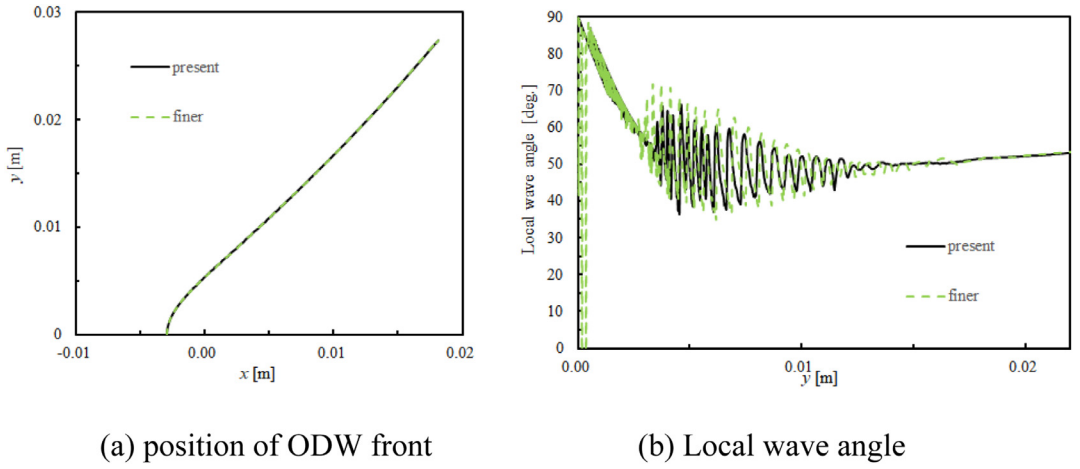

Fig. 6. Grid dependence of the location of ODW front and local wave angle for Φ_{out}=2.00 case (a) position of ODW front. (b) Local wave angle.

same way as in Fig. 4, where several incoming streamlines are denoted with Φ_{local} value. Written in the bracket of each caption is total equivalence ratio Φ_{total} in the whole domain. Thus, all the cases shown in Fig. 7 succeeded in the formation of ODW with curved wave front, which is due to a non-uniform detonation property and in agreement with [19]. Remembering the result of Φ=2.00 where SIC is formed, it is interesting to note that two cases of Φ_{out}=3.00 and 4.00 (Fig. 7(b)(e)) with fuel-rich composition in the outside (Hereafter, this is termed 'outer-rich' condition and 'outer-lean' for fuel-lean in the outside) retained ODW around the location of Φ_{local}=2.00. Moreover, the fact Φ_{total}>2.00 in the latter case is also worthy of attention, meaning increased chance for ODW initiation compared to uniform mixture. This observation combined with the success of all $\Phi_{\mathfrak{C}}$=1.00 cases in ODW formation as shown here in Fig. 7 prove that ODW initiation is primarily dependent on the value of $\Phi_{\mathfrak{C}}$, not on local equivalence ratio outside. And also, far from the sphere a broader range of mixture composition can experience ODW front. This could be partly due to a weaker effect of the scale of the sphere on attenuation of ODW downstream enough, replaced instead by dominance of curvature effect [8,36] and potential effect by the concentration gradient. Therefore, conventional explanation on the formation of ODW based on the scale ratio d/λ is indicated to be no longer valid away from the initiating body, and another indicator including the curvature [8,36] and newly involved factor of the concentration gradient should be taken into account.

Another important phenomenon to be noted here is the wave decoupling encountered near the outlet boundary in the case Φ_{out}=4.00 (Fig. 7(e) and enlarged by Fig. 7(f)), where detonation is quenched into decoupled SIC form. A discontinuous drop of the wave angle, and weak oscillating motion of the shock/flame fronts occurred involving higher-frequency behavior induced by transmitted transverse waves ~4 MHz and irregular lower-frequency motion of global wave corrugation on the order of several kHz. This decoupling phenomenon was similarily observed in our preceeding numerical work on different concentration gradients [37], and also our ongoing experiments on the same mixture $2H_2+O_2+3Ar$ (unpublished) observed in stronger concentration gradient. This decoupling occurred around Φ_{local}~2.8 in the present simulation, differently from above works (Φ_{local}~3.5 in [37] and Φ_{local}~1.8 in the experiment). Therefore, not only local composition but the strength of the gradient would influecnce onset of this critical phenomenon. In addition, the effect of numerical method including grid resolution should be taken into consideration for further quantitative discussion. This will be one of major concern in the comparative study involving corresponding experiments.

3.4. Local wave angle

In non-uniform mixtures simulated in Fig. 7, curved ODW front appeared in every case. There is a clear distinction between the outer-rich cases and outer-lean cases on whether convcave or convex wave is formed. This difference is simply attribtuted to dependence of detonation velocity on equivalence ratio, as represented by Fig. 3 as the calculation result of CEA on variable equivalence ratio of 2Φ H_2+O_2–3Ar mixture. Since increasing D_{CJ} towards fuel-rich composition means larger β_{CJ} through Eq. (1), these concaved/convex fronts

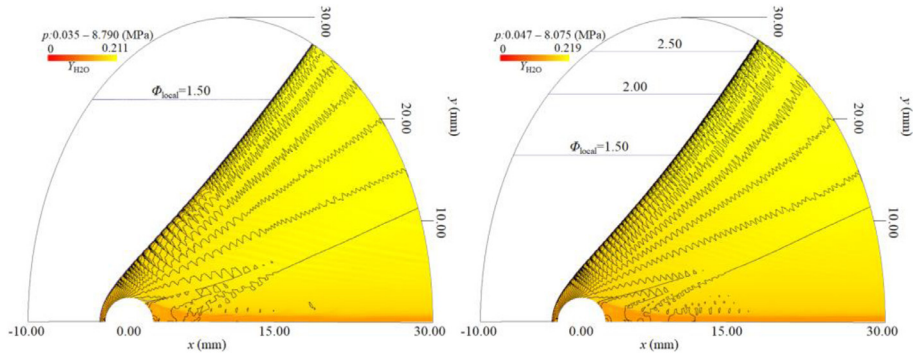

(a) Φ_{out}=2.00 (Φ_{tota}=1.45)

(b) Φ_{out}=3.00 (Φ_{tota}=1.83)

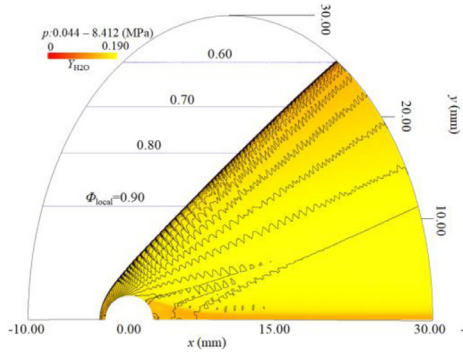

(c) Φ_{out}=0.50 (Φ_{tota}=0.71)

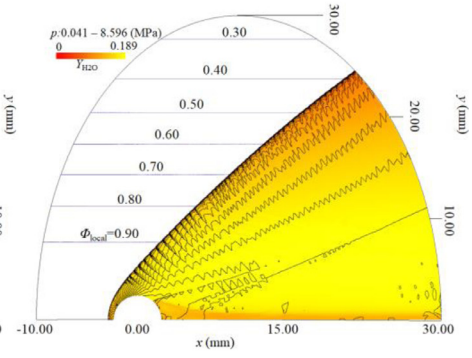

(d) Φ_{out}=0.25 (Φ_{tota}=0.51)

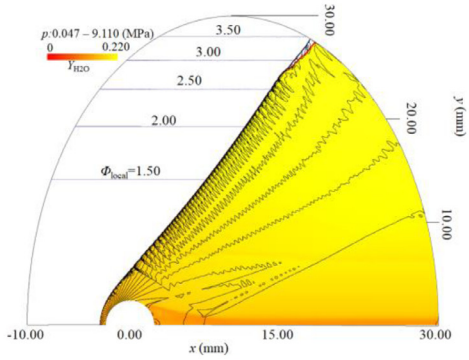

(e) Φ_{out}=4.00 (Φ_{tota}=2.16)

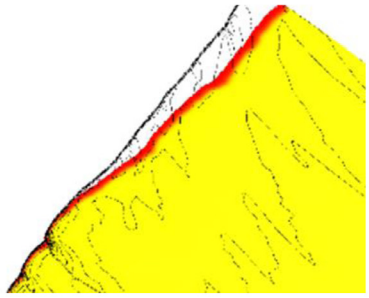

(f) Enlarged view of decoupled shock/flame in Φ_{out}=4.00 case

Fig. 7. Overlaid contours of pressure (black lines) and water mass fraction (color map) of non-uniform conditions. (a) Φ_{out}=2.00 (Φ_{tota}=1.45). (b) Φ_{out}=3.00 (Φ_{tota}=1.83). (c) Φ_{out}=0.50 (Φ_{tota}=0.71). (d) Φ_{out}=0.25 (Φ_{tota}=0.51). (e) Φ_{out}=4.00 (Φ_{tota}=2.16). (f) Enlarged view of decoupled shock/flame in Φ_{out}=4.00 case.

are considered to reflect theoretical detonation feature through the wave angle distributions.

Then, in order to investigate the correspondence of the local wave structure to C–J theory, a comparative analysis was conducted to track the local wave angles in each case and compute β_{CJ} of the local mixture by Eq. (1), in which D_{CJ} was calculated against variable equivalence ratio as shown in Fig. 3. The results for the cases from Fig. 7 are summarized in Fig. 8. Local equivalence ratio at each location on ODW or shock is taken to be the horizontal axis. Colored thin lines denote numerically predicted values, and a thick dashed line shows β_{CJ} calculated via detonation velocities predicted by the

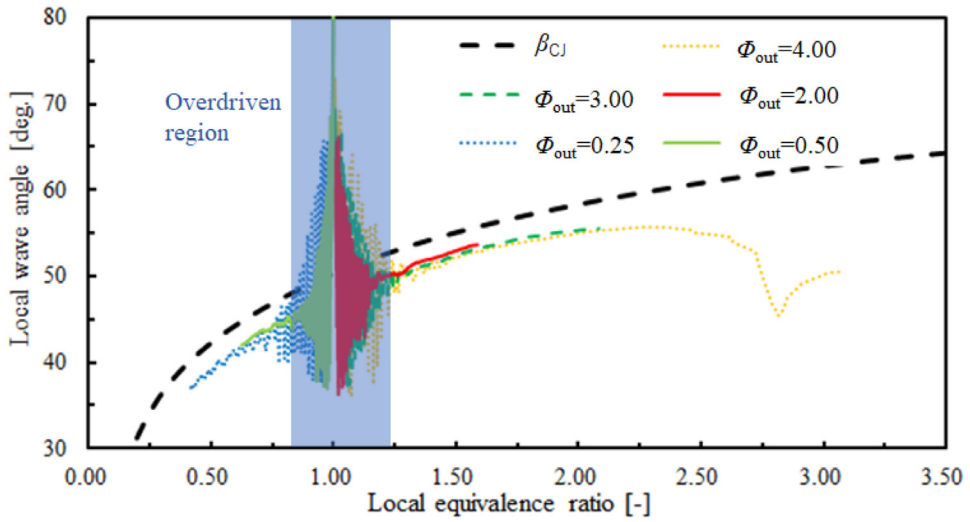

Fig. 8. Comparison of local wave angle observed in each non-uniform case with that calculation based on C–J theory.

CEA code. It is first noted that local wave angles in all the non-uniform cases clearly vary along analytical β_{CJ} values for the range $\Phi_{local}<2.00$, although the numerical values are always slightly lower (by a few degree 2–3°) as they were in the uniform $\Phi_{local}=1.00$ case. This is a reliable proof that self-sustained ODW retains its C–J theoretical properties even in a non-uniform mixture, despite the fact that C–J analysis is derived from one-dimensional flow assumption which should not be exact in essentially multi-dimensional non-uniform mixture flow.

However, exceptional behavior of the wave angle is found for $\Phi_{local}>2.00$, deviating slowly from C–J angle dependence. Around Φ_{local} ~2.3, the wave angle starts to decrease contrary to β_{CJ} dependence. Therefore, the decoupling phenomenon in this case is considered to initiate around this loation. A sudden drop around Φ_{local}~2.8 is followed by an oscillating behavior of shock angle due to the unsteady motion, keeping far lower than β_{CJ} value, which indicates detonation completely quenches in this region replaced by inert shock. The difference of the wave angle dependent on the magnitude of the concentration gradient was relatively weak compared to the effect of curvature and decoupling, but velocity deficit occuring in both outer-rich and outer-lean condition increases as the concentration gradient is increased with relatively minor magnitude <1.5°. Since curvature caused by the concentration gradient should affect in the opposite manner depending on whether outer-rich or outer lean condition is experienced, The same dependence in all concentration gradient towards lower detonation velocity indicates the need for consideration of the effect of concentration gradient.

A detailed view into a common trend found in the behavior for $\Phi_{out}=3.00$ and 4.00 implies that increasing trend of the wave angle starts to deviate from that of C–J angle around local equivalence ratio ~2.0. This common feature indicates that a slower kinetic rate due to fuel-rich composition also influences detonation velocity. Therefore, Not only curvature effeect as occurred in uniform mixture, but also composition far from stoichiometry and concentration gradient were both confirmed here to have influence on the static behavior of ODW to some extent.

4. Conclusion

Self-sustained oblique detonation wave (ODW) in a non-uniform hydrogen/oxygen/argon mixture was numerically investigated in an axisymmetric domain, prescribing the concentration gradient by the Gaussian distribution. A hypersonic combustible flow at 2500 m/s around a 4.76 mm diameter sphere body was modeled including a detailed kinetics of hydrogen–oxygen combustion. A first important result to be noted is that initiation of ODW is all successful when the centerline equivalence ratio is fixed to be unity, and also a broader range of local equivalence ratio can sustain oblique detonation away from the sphere. This result indicates the effect of wave attenuation by expansion wave is only strong close to the sphere, which alleviates the limitation of mixture composition in the outer region for detonation stabilization. Also, ODW in the non-uniformity was revealed to exhibit a curved wave front as was reported in the literature, whose local angle distribution mostly matched

1-D C–J solutions, but in a little lower value owing to curvature and potential effect of concentration gradient. ODW decoupling in the outside region was newly observed, which never occurred in a uniform mixture, accompanied by an abrupt change of the wave angle. This occurrence was associated with velocity deficit compared to C–J theory in strongly fuel-rich mixture, and is attributed to a slower kinetic rate. Although full explanation of the observed phenomena has not been reached at the present state, all these observed phenomena have never been reported before, shedding light onto the importance of studying the non-uniformity effects since these drastic changes can affect in favor or badly the engine operation and its performance.

Declaration of Competing Interest

None declared.

References

[1] R.A. Gross, *AIAA J.* 1 (5) (1963) 1225–1227.
[2] G.P. Menees, H.G. Adelman, J.L. Cambier, J.V. Bowles, *J. Propuls. Power* 8 (3) (1992) 709–713.
[3] P. Wolanski, *Proc. Combust. Inst.* 34 (1) (2013) 125–158.
[4] J. Chan, J.P. Sislian, D. Alexander, *J. Propuls. Power* 26 (5) (2011) 1125–1134.
[5] P.R. Ess, J.P. Sislan, C.B. Allen, *J. Propuls. Power* 21 (4) (2005) 667–680.
[6] H.F. Lehr, *Astronaut. Acta* 17 (1972) 589–597.
[7] S. Maeda, J. Kasahara, A. Matsuo, *Combust. Flame* 159 (2012) 887–896.
[8] S. Maeda, S. Sumiya, J. Kasahara, A. Matsuo, *Shock Waves* 25 (2015) 141–150.
[9] C. Li, K. Kailasanath, E.S. Oran, *Phys. Fluids* 6 (4) (1994) 1600–1611.
[10] L.F.F. da Silva, B. Deshaies, *Combust. Flame* 121 (2000) 152–166.
[11] H. Teng, Y. Zhang, Z. Jiang, *Comput. Fluids* 95 (2014) 127–131.
[12] J.-Y. Choi, E.J.-R. Shin, I.-S. Jeung, *Proc. Combust. Inst.* 32 (2) (2009) 2387–2396.
[13] J.-Y. Choi, D.-W. Kim, I.-S. Jeung, F. Ma, V. Yang, *Proc. Combust. Inst.* 31 (2007) 2473–2480.
[14] J. Verreault, A.J. Higgins, R.A. Stowe, *Proc. Combust. Inst.* 34 (2013) 1913–1920.
[15] W. Huang, S.L. Yan, Z. Wangm, *Acta Astronaut.* 84 (2013) 141–152.
[16] Y.W. Wang, J.P. Sislian, *J. Propuls. Power* 26 (5) (2010) 1114–1124.
[17] G.P. Menees, H.G. Adelman, J.L. Cambier, Analytical and Experimental Investigations of the Oblique Detonation Wave Engine Concept NASA TM-102839 (1991).
[18] J.P. Sislian, R. Dudebout, J.M.Islam Schumacher, T. Redford, *J. Propuls. Power* 16 (1) (2000) 41–48.
[19] J.L. Cambier, H. Adelman, G.P. Menees, *Jet Prop.* 6 (3) (1990) 315–323.
[20] V.V. Vlasenko, V.A. Sabel'nikov, *Combust. Explos. Shock Waves* 31 (3) (1995) 376–389.
[21] K. Ishii, M. Kojima, *Shock Waves* 17 (2007) 95–102.
[22] K.G. Vollmer, F. Ettner, T. Sattelmayer, *Combust. Sci. Technol.* 184 (2012) 1903–1915.
[23] J. Fujii, Y. Kumazawa, A. Matsuo, S. Nakagami, K. Matsuoka, J. Kasahara, *Proc. Combust. Inst.* 36 (2017) 2665–2672.
[24] S. Boulal, P. Vidal, R. Zitoun, *Combust. Flame* 172 (2016) 222–233.
[25] K. Iwata, S. Nakaya, M. Tsue, *AIAA J.* 54 (5) (2016) 1682–1692.
[26] K. Iwata, S. Nakaya, M. Tsue, *Trans. Jpn. Soc. Aeronaut. Space Sci. Technol.* 14 (ists30) (2016) 31–38.
[27] K. Iwata, S. Nakaya, M. Tsue, *Proc. Combust. Inst.* 36 (2017) 2761–2769.
[28] K. Iwata, K. Tomita, I. Yoshiki, et al., *J. Combust. Soc. Jpn.* 60 (192) (2018) 124–132 (published in Japanese).
[29] Y. Fang, Z. Hu, H. Teng, Z. Jiang, H.D. Ng, *Aero. Sci. Technol.* 71 (2017) 256–263.
[30] M. Baum, T.J. Poinsot, D. Thevenin, *J. Comput. Phys.* 176 (1994) 247–261.
[31] A.A. Konnov, *Eurasian Chem. Technol. J.* 2 (2000) 257–264.
[32] M.-S. Liou, *J. Comput. Phys.* 214 (2006) 137–170.
[33] C.W. Shu, S. Osher, *J. Comput. Phys.* 77 (2) (1988) 439–471.
[34] N. Tsuboi, K. Hayashi, *J. Jpn. Soc. Fluid Mech. Nagare* 26 (2007) 183–192 (published in Japanese).
[35] B.J. McBride, M.J. Zehe, S. Gordon, *Chemical Equilibrium with Applications*, NASA Glenn Research Center, 2010.
[36] S. Maeda, S. Sumiya, J. Kasahara, A. Matsuo, *Proc. Combust. Inst.* 34 (2013) 1973–1980.
[37] K. Iwata, S. Nakaya, M. Tsue, in: Proceedings of the 26th International Colloquium on the Dynamics of Explosions and Reactive Systems (26th ICDERS), Boston, USA, The Combustion Institute, 2017, p. 1009.